

# Preparation and characterization of antibacterial films based on polyvinyl alcohol/quaternized cellulose



Dongying Hu, Lijuan Wang\*

Key Laboratory of Bio-based Material Science and Technology of Ministry of Education, Northeast Forestry University, 26 Hexing Road, Harbin 150040, China

## ARTICLE INFO

### Article history:

Received 18 June 2015

Received in revised form 11 February 2016

Accepted 28 February 2016

Available online 2 March 2016

### Keywords:

Poly(vinyl alcohol)

Quaternized cellulose

Regenerated composite film

Antibacterial activity

Physical property

## ABSTRACT

Quaternized cellulose (YM) was homogeneously synthesized by grafting 3-chloro-2-hydroxypropyl dodecyldimethylammonium groups onto cellulose molecules in a NaOH/urea aqueous solution. YM was blended with a poly(vinyl alcohol) (PVA) matrix to prepare composite films via co-regeneration from the alkaline solution. The PVA film and the blend films were characterized by Fourier transform infrared spectroscopy, X-ray diffraction measurements, thermogravimetric analysis, and scanning electron microscopy. Mechanical properties, water vapor barrier properties, light transmission, and antibacterial activity against Gram-positive (*Staphylococcus aureus*) and Gram-negative (*Escherichia coli*) bacteria were also evaluated. The results reveal that PVA and YM in the composite films interacted by hydrogen bonding. Compared with pure PVA film, the PVA/YM blend films had higher tensile strength, higher thermostability, lower water permeability, and especially, higher antibacterial activity. The blend films exhibited good UV-shielding performance. Our study demonstrates a simple and efficient method for preparing a functional, environment-friendly composite film.

© 2016 Published by Elsevier B.V.

## 1. Introduction

The massive use of non-degradable plastic materials has caused serious “white pollution”. Many efforts have been made to develop environment-friendly biomaterials to solve environmental problems while reducing the dependence on petroleum-based fuel and products. Cellulose, a natural polymer, has become an attractive solution to the increasing demand for environment-friendly and biocompatible materials [1,2]. Many works have intensively investigated materials from regenerated cellulose films because of their high mechanical strength, thermal stability, biocompatibility, and nontoxicity [3–6]. However, pure regenerated cellulose films are highly hydrophilic, have poor barrier properties, and lack antimicrobial activity. These characteristics have limited their potential applications [7–9]. Chemical modification or combination with other polymers effectively overcomes these problems.

Poly(vinyl alcohol) (PVA) is a highly biocompatible, nontoxic synthetic polymer with high water solubility. It can be blended with other natural polymers to produce biodegradable composites. It has promising industrial applications in many fields because of its film-forming, emulsifying, and adhesive properties [10–12]. PVA films have remarkable barrier properties due to their small, dense, and closely packed monoclinic crystal structure. Cellulose is often used as reinforcement filler for PVA. However, cellulose-reinforced PVA-based films have

limited application in functional packaging because of their lack of antibacterial activity. Thus, improving the antimicrobial activity of PVA-based composite films is of importance.

The use of natural and synthetic antibacterial agents is considered as a promising approach to control the growth of microorganisms [13]. Antibacterial agents include nanometal or metal oxides [14,15], antibiotics, halogens [16], and essential oils from herbs and spices [17]. However, there are several disadvantages associated with the use of these antibacterial agents. Use of nanometal or metal oxides, antibiotics, and halogens can readily lead to secondary pollution. The antibacterial activity of essential oils is transient because of their volatility. On the other hand, quaternary ammonium compounds are widely used because of their antibacterial properties, low toxicity, low cost, and environmental compatibility [18]. They have recently been used to modify cellulose derivatives used as bioadsorbents, flocculants, and gene carriers [19,20]. However, there are no reports on the incorporation of quaternized cellulose (YM) in the preparation of antibacterial films with PVA as matrix.

In the present study, 3-chloro-2-hydroxypropyl dodecyldimethylammonium chloride (YB) was synthesized through a reaction between *N,N*-dimethyl-1-dodecylamine and epichlorohydrin (EH) in alkali/urea aqueous solution. The obtained YB was used to modify cellulose for synthesis of the quaternized cellulose (YM). The PVA/YM composite films were regenerated from the alkali/urea aqueous solution. YM, PVA film, and YM/PVA films were characterized by Fourier transfer infrared (FTIR) spectroscopy, X-ray diffraction (XRD) measurements, thermogravimetric analysis (TGA), scanning electron microscopy, tensile tests, oxygen permeability (OP) measurements, water vapor permeability (WVP) tests, and light-transmission measurements. Their activity against

\* Corresponding author.

E-mail address: [donglinwj@163.com](mailto:donglinwj@163.com) (L. Wang).

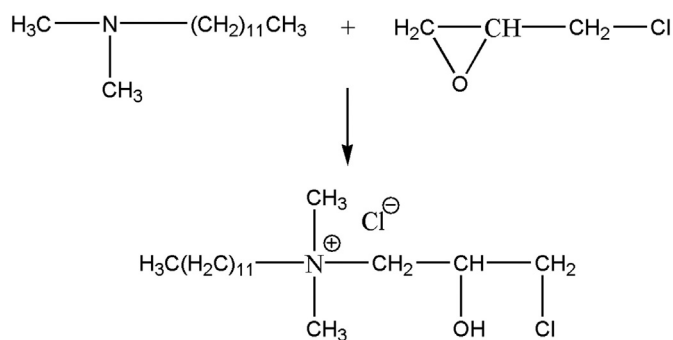


Fig. 1. Synthetic reaction for the YB.

Gram-positive (*Staphylococcus aureus*) and Gram-negative (*Escherichia coli*) bacteria were also investigated.

## 2. Materials and methods

### 2.1. Materials

Microcrystalline cellulose (MCC, Comprecel M101; degree of polymerization (DP) = 200), was purchased from Shanghai Shenmei Pharmaceutical Technology Co., Ltd. (Shanghai, China). PVA (average molecular weight  $M_w = 84,000$ – $89,000$ ; DP = 1700–1800; degree of hydrolysis = 88%) was purchased from Sinopec Shanghai Petrochemical Co., Ltd. (Shanghai, China). *N,N*-Dimethyl-1-dodecylamine ( $\text{C}_{14}\text{H}_{31}\text{N}$ ; 98% pure;  $M_w = 213.4$ ) was obtained from Heowns Chemical Reagent Co. Ltd. (Tianjin, China). All other reagents and solvents were of analytical grade and were used as received. The microorganisms used in this study were obtained from Qingdao Hope Bio-Technology Co., Ltd. (Qingdao, China) and were stored at  $4^\circ\text{C}$  before use. Biochemical reagents for the nutrient agar were purchased from AoBoXing Bio-tech Co., Ltd. (Beijing, China).

### 2.2. Preparation of blend films

#### 2.2.1. Preparation of YB

YB was synthesized from *N,N*-dimethyl-1-dodecylamine and EH. EH solution (219 mL, 2.79 mol) was added dropwise to a 300 mL (1.11 mol)

solution of *N,N*-dimethyl-1-dodecylamine [21]. The mixture was stirred at  $60^\circ\text{C}$  for 2 h to obtain a highly viscous solution, and the residual EH was removed by a procedure using vacuum–rotary evaporation. After the product was cooled to room temperature, it was dissolved in acetone (500 mL). Crystals began to separate in a few minutes. After the mixture was stored for 8 h at  $25^\circ\text{C}$ , it was filtered. The crystal-like products were washed with diethyl ether and then dried at  $60^\circ\text{C}$  under vacuum for 24 h. The product obtained was labeled as YB. The yield was 76% which approximated to the yield of 77% in the reference [21]. The reaction involved in this process is shown in Fig. 1. Results of its analysis are given below:

Elemental analysis (YB,  $\text{C}_{17}\text{H}_{37}\text{Cl}_2\text{NO}$ ). Measured (%): N 4.14%, C 59.73%, H 10.86%; calculated (%): N 4.09%, C 59.65%, H 10.82%.

YB:  $^1\text{H}$  nuclear magnetic resonance spectrometer ( $^1\text{H}$  NMR) ( $\text{D}_2\text{O}$ , 300 MHz):  $\delta$  0.75 (t, 3H,  $J = 3.75$ ), 1.16 (q, 18H,  $J = 8.2$ ), 1.57 (q, 2H,  $J = 7.8$ ), 3.20 (s, 6H), 3.45 (t, 2H,  $J = 4.8$ ), 4.15 (d, 2H,  $J = 2.4$ ), 6.18 (d, 2H,  $J = 8.4$ ), 6.29 (q, 1H,  $J = 2.8$ ).

#### 2.2.2. Preparation of YM

A cellulose solution was prepared according to a previously reported method [22]. Predetermined amounts of NaOH, urea, and distilled water (7:12:81 by weight) were combined in a 100 mL beaker to obtain a solution. MCC (2 g) was dispersed in the NaOH/urea solution, which was then cooled to  $-12.5^\circ\text{C}$ . The frozen mixture was then thawed and vigorously stirred for 5 min at ambient temperature to obtain a transparent solution of 2 wt.% cellulose. A specified amount of YB was added to the cellulose solution, and the mixture was stirred at  $25^\circ\text{C}$  for 24 h. The mole ratio of YB to anhydroglucose units in the cellulose molecules was 6:1. The resulting solution of quaternized MCC derivative was separated into two parts. One was used to obtain the purified quaternized MCC derivative (YM) [23] for further analysis. The other was stored at  $0^\circ\text{C}$  for direct use in the preparation of YM/PVA blend films. The possible synthesis scheme of YM is shown in Fig. 2.

#### 2.2.3. Preparation of YM/PVA blend films

PVA was stirred into distilled water at  $80^\circ\text{C}$  for 2 h to achieve a clear PVA solution (8.80%). Specified amounts of PVA and YM solution were mixed, and the resulting solution was stirred vigorously for 30 min. After the solution was degassed in a vacuum oven, it was spread onto a glass sheet to form a gel with a thickness of  $\sim 0.2$  mm. The sheet was immersed in a coagulation bath containing of 5 wt.%  $\text{CaCl}_2$  and 3 wt.%

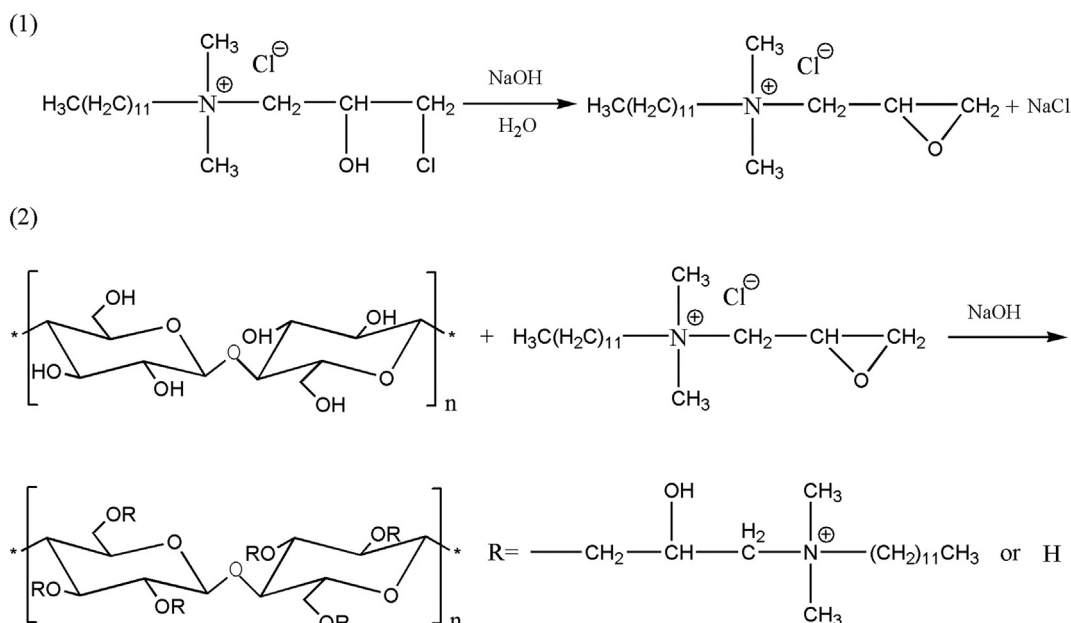


Fig. 2. Synthetic reactions for the YM.

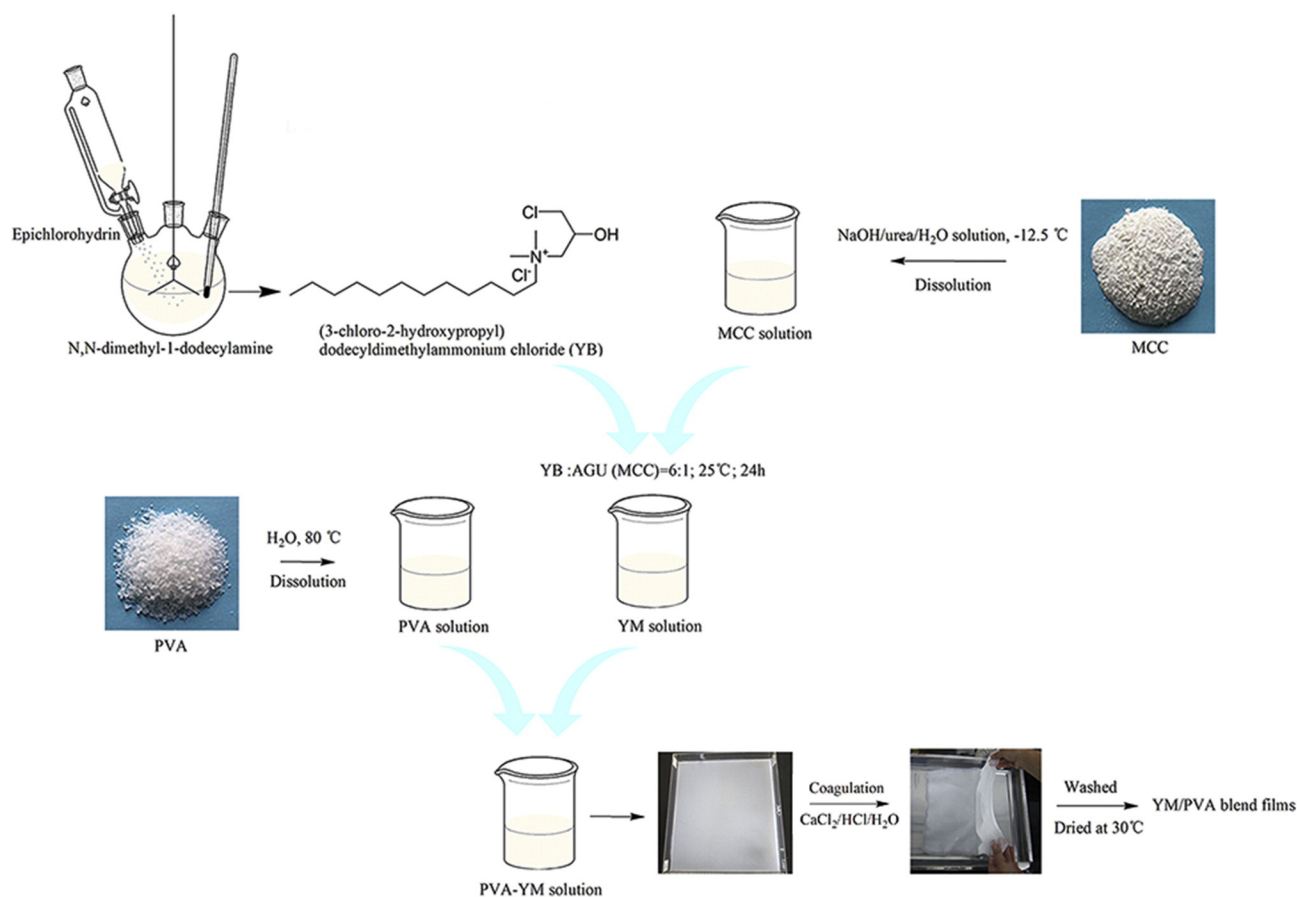


Fig. 3. Process of preparation of the PVA/YM composite films.

HCl at 25 °C for 10 min to obtain regenerated YM/PVA blend films with uniform thickness. The films were washed with running water and then with deionized water. The wet films were then fixed onto a polyvinyl chloride (PVC) sheet to prevent shrinkage and finally air-dried at 25 °C. The blend films, denoted as YMP-5, YMP-10, YMP-15, and YMP-20, contained 5, 10, 15, and 20 wt.% YM, respectively. The control (PVA film) was obtained through the above process but without

addition of YM solution. The preparation procedure for the blend films is shown in Fig. 3.

### 2.3. Characterization

FTIR spectra of the films were obtained on a Nicolet 6700 spectrometer (Thermo Fisher Scientific Co., Ltd., MA, USA). Measurements were

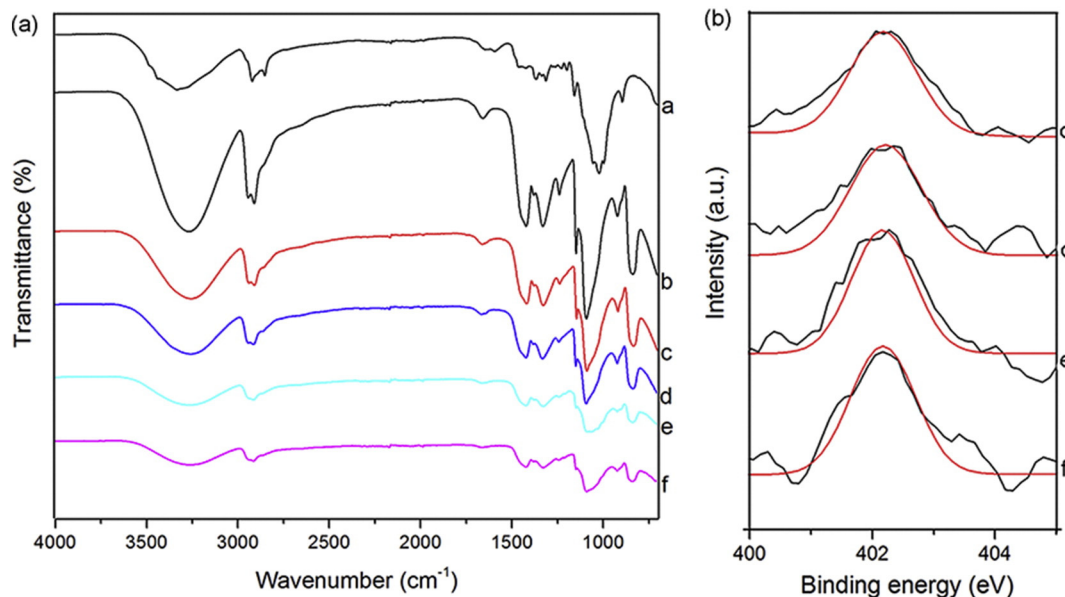


Fig. 4. FTIR spectra of (a) YM, (b) PVA, (c) YMP-5, (d) YMP-10, (e) YMP-15, and (f) YMP-20. (b) N1s XPS spectra of YMP films.

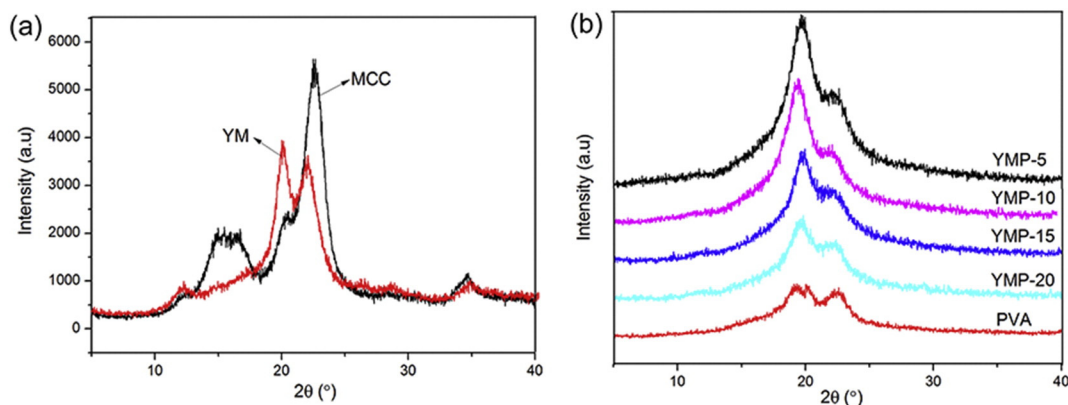


Fig. 5. X-ray diffraction patterns of (a) MCC, quaternized MCC (YM), and (b) PVA, YMP-5, YMP-10, YMP-15, and YMP-20 films.

done in attenuated total reflection mode at a resolution of  $4\text{ cm}^{-1}$  in a range of wavenumber from  $4000$  to  $700\text{ cm}^{-1}$ . These films were dried at  $40\text{ }^{\circ}\text{C}$  for 24 h and cut into  $1\text{ cm} \times 1\text{ cm}$  before the measurement.  $^1\text{H}$  NMR spectrum was recorded on a spectrometer (AVANCE DRX-500, Bruker, Germany), operating at 300 MHz. XRD patterns of the films were obtained by using a D/max-2200 diffractometer ( $\text{Cu-K}\alpha$  target, 40 kV, 30 mA) operated at 1200 W (Rigaku, Japan) with a scanning rate of  $5^{\circ}/\text{min}$  and the scanning scope of  $2\theta$  ( $5\text{--}40^{\circ}$ ) at ambient temperature. The nitrogen content (N%) was measured on an element analyzer (EA 3000, Arvator, Italy), and the valence state of nitrogen in the composite films was determined by using a K-Alpha X-ray photoelectron spectroscopy (XPS) analyzer (Thermo Fisher Scientific Company, USA). The morphology of the films was examined under a Quanta 200 scanning electron microscope (Philips-FEI Co., AMS, The Netherlands) with an accelerating voltage of 5 kV. Prior to the observation, the films were frozen in liquid nitrogen and snapped immediately to prepare the sample of upper surface and cross-sections, then, the samples were coated with a thin gold layer. TGA of the films was carried out on a TA Instruments TGA Q500 (TA Instruments, USA) with a heating rate of  $10\text{ }^{\circ}\text{C}/\text{min}$  in the temperature range from  $30\text{ }^{\circ}\text{C}$  to  $600\text{ }^{\circ}\text{C}$  and the nitrogen flow of  $20\text{ mL}/\text{min}$ . Brunauer–Emmett–Teller (BET) surface areas of samples were measured by using a JW-BK132F instrument (JWGB Sci. & Tech. Co., Ltd., Beijing, China). Films thicknesses were measured with an ID-C112XBS micrometer (Mitutoyo Corp., Tokyo, Japan) and reported as the average from ten points. The OP and WVP of the films were determined at  $30\text{ }^{\circ}\text{C}$  by using a Perme OX2/230 (Lab-think, Jinan, China) according to ASTM D3985-05 (2002), and a Mocon Permatran-W 3/61 (MOCON, MN, USA) according to GB/T 26253 (GB/T, 2010), respectively. Tensile tests were performed on the films at a strain rate of  $300\text{ mm}/\text{min}$  at  $25\text{ }^{\circ}\text{C}$  by using an

auto tensile tester (XLW-PC, Param, Jinan, China) equipped with a 500 N load cell. The film specimens had width and length of 10 and 150 mm, respectively. Light transmission through the blend films ( $4\text{ cm} \times 3\text{ cm}$ ) was measured on an ultraviolet–visible (UV–vis) spectrophotometer (UV-2600, Shimadzu, Kyoto, Japan) in the range of  $800\text{--}200\text{ nm}$ .

#### 2.4. Antibacterial activity

Antimicrobial activities of the films were assessed by measuring the inhibition zone around each disc of film. Bacteria were grown in nutrient broth (NB) liquid medium at  $37\text{ }^{\circ}\text{C}$  for 12 h and further diluted to obtain a concentration of  $\sim 10^8\text{ CFU}/\text{mL}$ . Dilute suspensions (0.1 mL) of *E. coli* and *S. aureus* were separately combined with nutrient agar (NA) agar medium. Control films (PVA) and YMP films were used. The films were cut into circular discs 8 mm in diameter, and were centrally placed on the solid agar plates inoculated with the test bacteria. Each agar plate was incubated at  $37\text{ }^{\circ}\text{C}$  for 24 h before examination for clear zones around test materials. Clear zones are sites where bacterial growth was inhibited. Three replicate tests were carried out under the same conditions for each sample.

#### 2.5. Statistical analysis

Multiple samples were tested, and all data were reported are average values  $\pm$  standard deviation. The statistical analysis was done by one way analysis of variance (ANOVA) using SPSS software, and differences among mean values were processed by Duncan's multiple-range tests. Significance was determined at  $p$  values of  $<0.05$ .

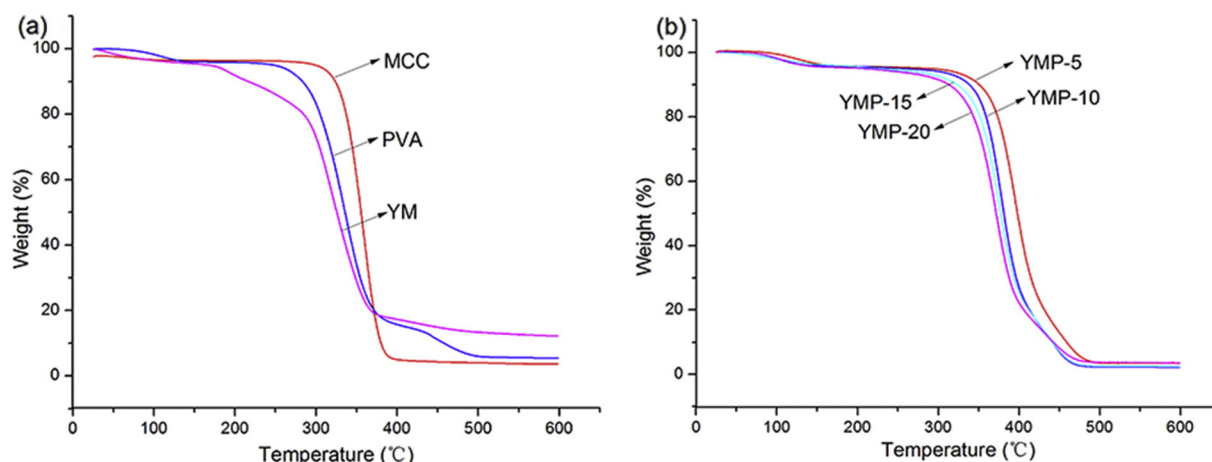
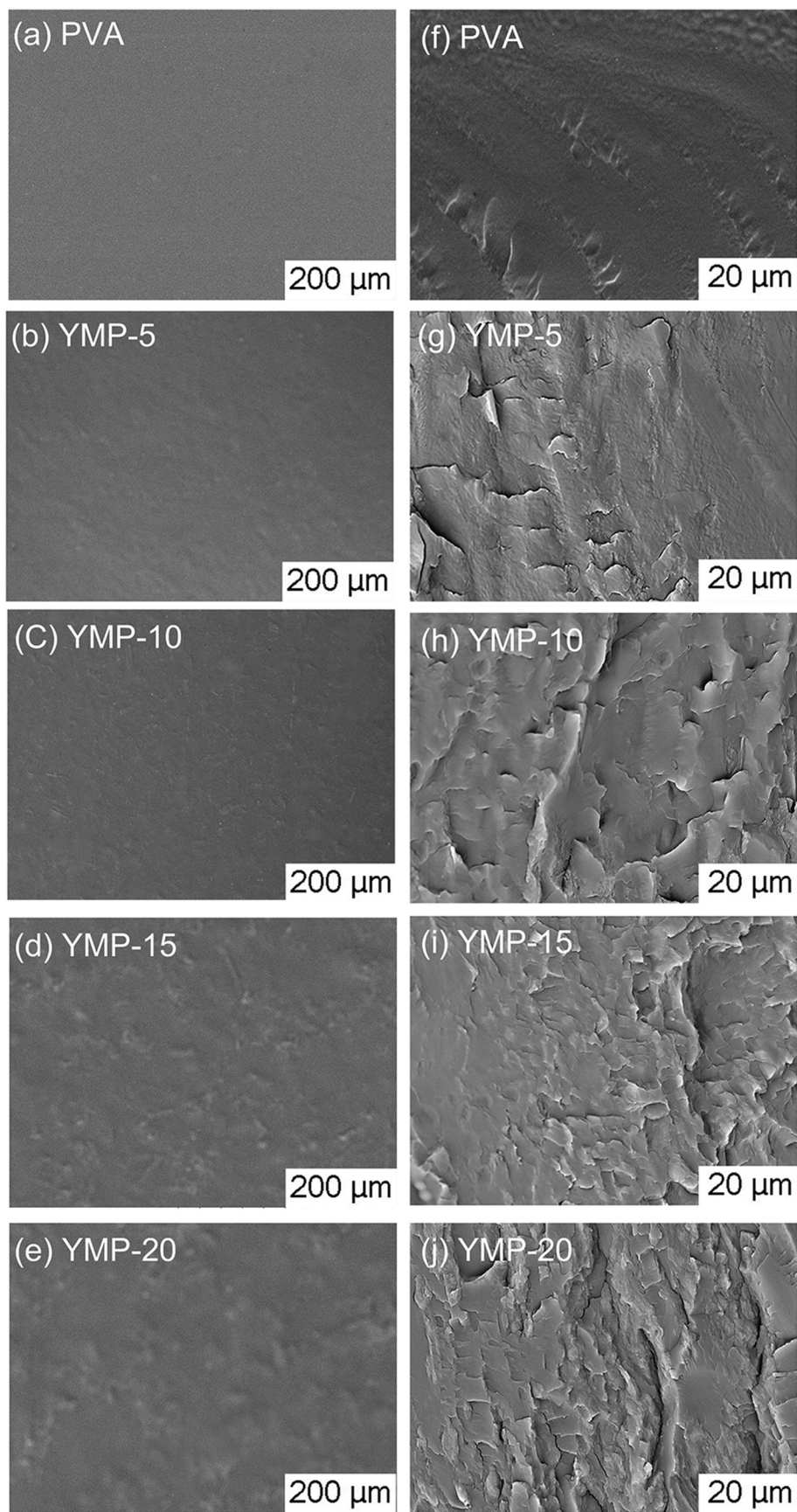


Fig. 6. Thermograms of (a) MCC, PVA, YM, and the blend films (b) YMP-5, YMP-10, YMP-15, and YMP-20.



**Fig. 7.** SEM micrographs of the surfaces (a–e) and cross sections (f–j) of the films.

### 3. Results and discussion

#### 3.1. FTIR spectroscopy

FTIR spectroscopy, a common method for studying the structural and chemical properties of materials, was performed (results are shown in Fig. 4(a)). Bands for YM appeared at  $3339\text{ cm}^{-1}$  (O–H stretching), at  $2921$  and  $2854\text{ cm}^{-1}$  ( $\nu_{\text{as}}(\text{CH}_2)$ ,  $\nu_{\text{s}}(\text{CH}_2)$ ), as well as at  $1310$ ,  $1102$ ,  $1024$ , and  $895\text{ cm}^{-1}$  (glucopyranose ring). The band at  $1456\text{ cm}^{-1}$  is due to the introduction of C–N<sup>+</sup>–C in the structure, which indicates the formation of YM [24]. The degree of substitution of YM from element analysis is 0.48, which further supports the above results. Characteristic peaks of PVA film could be observed at  $3283\text{ cm}^{-1}$  (O–H stretching),  $2913\text{ cm}^{-1}$  (C–H bending),  $1732\text{ cm}^{-1}$  (CO stretching), and  $1086\text{ cm}^{-1}$  (C–O stretching) [25]. Characteristic bands of PVA in the YMP films are apparent; however, characteristic bands of YM almost overlap. As shown in Fig. 4(b), the peak at  $\sim 402.23\text{ eV}$  in the XPS spectra is consistent with nitrogen in quaternary ammonium groups [26], which further confirms the introduction of YM into the blend films. Furthermore, the O–H stretching vibration bands of the YMP blend films at  $3260\text{--}3240\text{ cm}^{-1}$  broadened and shifted to lower wavenumber, indicating the strong intermolecular hydrogen bonding between YM and PVA in the blend films [27]. The interaction between PVA and YM thus increased the tensile strength of the blend films.

#### 3.2. XRD analysis

XRD measurement is commonly used to investigate the crystalline nature of materials. As shown in Fig. 5, characteristic peaks of MCC are located at  $2\theta$  values of  $14.9^\circ$ ,  $16.4^\circ$ ,  $22.6^\circ$ , and  $34.6^\circ$ , which correspond to the typical structure of cellulose I. However, weaker peaks of YM at  $2\theta$  values of  $12.3^\circ$ ,  $20.1^\circ$ , and  $22.0^\circ$  represent the structure of cellulose II. These changes indicate that cellulose molecules rearranged and that the cellulose I structure transformed to cellulose II structure during quaternization and subsequent regeneration from the NaOH/urea solution. Peaks of pure PVA film at  $2\theta$  values of  $19.2^\circ$  and  $22.1^\circ$  are characteristic of the structure of crystalline PVA. Furthermore, peaks of the YMP films at  $2\theta$  values of  $19.5^\circ$  and  $22.4^\circ$  are close to those of the PVA film. The intensities of the peaks of YMP films are greater than those of pure PVA film. These results indicate that hydrogen bonds between PVA and YM in the blend films were strong. However, the intensity of the peak at  $2\theta$  value of  $19.5^\circ$  markedly decreased upon addition of YM. During regeneration, greater amounts of urea, which came from the NaOH/urea aqueous solution used during film preparation, remained in the blend film as the YM content increased. –OH, CO and –NH<sub>2</sub> groups in urea could form hydrogen bonds with hydroxyl groups of YM or PVA molecules, which hindered the primary interactions between hydroxyl groups in YM or PVA molecules. Meanwhile, the decreased dispersion of YM with the increase in YM content of the blend films could also lead to lower crystallinity.

#### 3.3. TGA

Fig. 6 shows thermograms of MCC, YM, neat PVA film, and PVA/YM composite films. As shown in Fig. 6(a), the major degradation temperature of MCC was  $331.11^\circ\text{C}$ , which is higher than that of YM ( $283.74^\circ\text{C}$ ). This difference indicates that the thermal stability of MCC decreased after the modification. The weight loss of PVA observed at  $83^\circ\text{C}$  is attributed to moisture removal, and the two subsequent major weight losses within  $220\text{--}500^\circ\text{C}$  could be attributed to structural decomposition and to the release of acetyl groups from PVA [28]. Thermograms of the YMP films (YMP-5, YMP-10, YMP-15, and YMP-20) are shown in Fig. 6(b). The initial weight loss observed at  $\sim 90^\circ\text{C}$  is due to water evaporation. Subsequent major degradation occurred at temperatures of  $368.40$ ,  $354.38$ ,  $348.74$  and  $342.59^\circ\text{C}$ , which are all higher than those of PVA

or of YM. These results further suggest the strong interaction between YM and PVA, which enhanced the thermostability of the blend films [29]. However, the onset decomposition temperature and the major decomposition temperature of the PVA/YM composite films markedly shifted to lower temperature as the YM content increased from 5 to 20 wt.%. The decrease in thermal stability of PVA with increasing amount of incorporated YM may be explained by the decrease in compatibility between YM and PVA matrixes and by the decrease in crystallinity of the composite film. These conclusions are strongly supported by the XRD results.

#### 3.4. Morphology of PVA and YMP films

SEM images of the upper surfaces and cross sections of the films are shown in Fig. 7. The surface of the PVA film was homogeneous, but its cross section is heterogeneous because of the coexistence of crystalline and amorphous regions [30]. The YMP films had a microstructure that was rougher than of the PVA films; phase separation occurred when the YM content increased from 5% to 20%. These observations suggest that PVA and YM became more incompatible with the increase in YM content. Therefore, YM was miscible with PVA, and both formed a uniform film at low YM concentrations.

#### 3.5. Mechanical properties

The mechanical properties of samples are presented in Table 1 ( $p < 0.05$ ). The tensile strength and elongation at break of the PVA film are  $28.83 \pm 1.04\text{ MPa}$  and  $331.48\% \pm 2.57\%$ , respectively. The tensile strengths of YMP-5, YMP-10, YMP-15, and YMP-20 were higher than that of the PVA film but had relatively short elongation at break. This result implies that addition of YM to the films could improve their mechanical properties by causing the formation of strong hydrogen bonds between PVA and YM. The tensile strength of YMP-5 was higher than those of cellulose/PVA film ( $29\text{ MPa}$ ) [31], 5 wt.% NFC/PVA film ( $44.25\text{ MPa}$ ) [32], 7 wt.% CN/starch/PVA film ( $19.5\text{ MPa}$ ) [33], 32 wt.% of  $\alpha$ -CNFs/PVA ( $39\text{ MPa}$ ) [34], and 50 wt.% cellulose/PVA film ( $20\text{ MPa}$ ) [35]. The tensile strength decreased and the elongation at break increased with increasing YM content because of the decreased YM dispersion. It may also be due to the residual urea from regeneration of the YMP films, which reduced the degree of crystallinity. These observations also reveal that addition of YM decreased the elasticity of PVA film.

#### 3.6. Barrier properties

The gas permeability of packaging materials is of great importance to their use in preservation. A packaging system's barrier to oxygen can extend product shelf life and thus improve product quality [36]. All of our films had low OP, implying that they had high imperviousness toward oxygen. Moreover, the OP values of YMP films obtained in this work were lower than those of some polymer films, such as methyl cellulose [37], native and denatured whey protein isolate [38], calcium-crosslinked peach puree [39], high or low density polyethylene [40],

**Table 1**  
Mechanical properties of the films.

Sample	$\sigma_b$ (MPa)	$\epsilon_b$ (%)
PVA	$28.83 \pm 1.04e$	$331.48 \pm 2.57a$
YMP-5	$82.97 \pm 0.70a$	$52.08 \pm 0.64e$
YMP-10	$72.82 \pm 1.15b$	$58.04 \pm 1.31d$
YMP-15	$45.35 \pm 0.71c$	$62.52 \pm 1.28c$
YMP-20	$37.87 \pm 0.85d$	$65.32 \pm 1.62b$

Values are expressed as mean  $\pm$  standard deviation. Different letters in the same column indicate significant differences ( $p < 0.05$ ).

**Table 2**  
BET surface areas and barrier properties of PVA and YMP films.

Sample	$S_{\text{BET}}$ ( $\text{m}^2 \text{g}^{-1}$ )	$OP \times 10^{-6}$ ( $\text{cm}^3 \text{mm m}^{-2} \text{atm}^{-1} \text{day}^{-1}$ )	$WVP \times 10^{-8}$ ( $\text{g cm}^{-1} \text{s}^{-1} \text{Pa}^{-1}$ )
PVA	$1.94 \pm 0.32\text{d}$	$2.48 \pm 0.29\text{e}$	$25.82 \pm 1.84\text{d}$
YMP-5	$2.92 \pm 0.59\text{c}$	$4.50 \pm 0.54\text{d}$	$9.73 \pm 0.80\text{d}$
YMP-10	$3.38 \pm 0.26\text{c}$	$6.81 \pm 0.50\text{c}$	$11.7 \pm 1.74\text{d}$
YMP-15	$4.37 \pm 0.23\text{b}$	$8.60 \pm 0.48\text{b}$	$16.03 \pm 1.50\text{c}$
YMP-20	$7.22 \pm 0.42\text{a}$	$12.67 \pm 1.45\text{a}$	$21.77 \pm 1.53\text{b}$

Data are derived from the results of three independent experiments and are expressed as mean  $\pm$  standard deviation. Different letters in the same column indicate significant differences ( $p < 0.05$ ).

and chitosan [41]. The BET surface area and OP of the YMP films increased with the increase in YM content. A larger BET surface area corresponds to a structure with more pores, which increases the oxygen gas permeance. Moreover, the hydrogen bonds between the PVA and YM molecular chains become stronger as the crystallinity of the film increases. This further hinders passage of  $\text{O}_2$  through the film [42].

In general, water vapor transmission through a hydrophilic film depends on the diffusivity and solubility of water molecules in the film [43]. Water vapor barrier properties of the films as determined by the WVP are shown in Table 2 ( $p < 0.05$ ). Films with greater hydrophilicity have greater WVP (i.e., they have a lower barrier against water vapor). The WVP of PVA film is  $25.82 \pm 1.84 \times 10^{-8} \text{ g cm}^{-1} \text{ s}^{-1} \text{ Pa}^{-1}$ . Thus, addition of YM to PVA film had a marked effect on the water vapor barrier properties of the films compared with those of PVA film. The WVP values of YMP films reached a minimum of  $9.73 \pm 0.80 \times 10^{-8} \text{ g cm}^{-1} \text{ s}^{-1} \text{ Pa}^{-1}$  when the YM content was 5 wt%. This minimum indicates that a strong interaction existed between YM and PVA molecules and that the water vapor barrier properties of the PVA matrix improved upon the addition of YM. The WVP values of YMP films obtained in this work were higher than those of hydrophobic polymeric films such as PVA, LDPE, and HDPE [44]. However, the WVP value of YMP-5 was lower than those of chitosan and chitosan-cinnamon leaf oil films reported by Perdones

et al. [45], urea/PVA/xylan and glycerol/PVA/xylan composite films reported by Wang et al. [46]. At YM content higher than 5 wt%, the WVP values increased with increasing of YM content. This trend may also be attributed to the hydrophilic nature of YM and the lower crystallinity of the blend film.

### 3.7. UV transmittance of the composite films

Photographs of the films and UV-vis spectra of PVA and YMP films with  $68 \pm 4 \mu\text{m}$  thicknesses are presented in Fig. 8 ( $p < 0.05$ ). The PVA film was relatively transparent; its transmittance reached  $77.43 \pm 0.74\%$  at 280 nm. In contrast, the transparency of YMP-5 film was  $43.65 \pm 0.60\%$ ; an object on the other side of the film appeared hazy. Increasing the YM content from 5 to 10 wt.% drastically decreased the light transmittance. The transmittance at 280 nm was only  $0.03 \pm 0.01\%$  at YM content of 20 wt.%. The blend film became completely opaque at YM concentrations of 10, 15, and 20 wt.%. The film gradually became whiter, completely obscuring the object underneath it. The decreased transmittance is related to the decreased dispersion and to the increased incompatibility between YM and PVA at higher YM content. These in turn increase the number of interfaces in the blend films, leading to optical scattering and refraction. The above results indicate that YM plays an important role in blocking UV light through the films. Therefore, composite films have potential application in UV-screening materials.

### 3.8. Antibacterial properties

The antibacterial activity of the composite films was determined by disc diffusion method. Fig. 9 shows the effects of the films against Gram-positive (*S. aureus*) and Gram-negative (*E. coli*) bacteria ( $p < 0.05$ ). The control films (PVA) did not have a surrounding inhibition zone, suggesting that PVA film had no antibacterial activity. In contrast, the YMP film disc had a clear inhibition zone around it, indicating an antibacterial effect. The antibacterial component in the blend films diffused to the surrounding area of the film, suppressing the growth of *E. coli* and *S. aureus* and thus forming an inhibition zone around the film. Quaternary

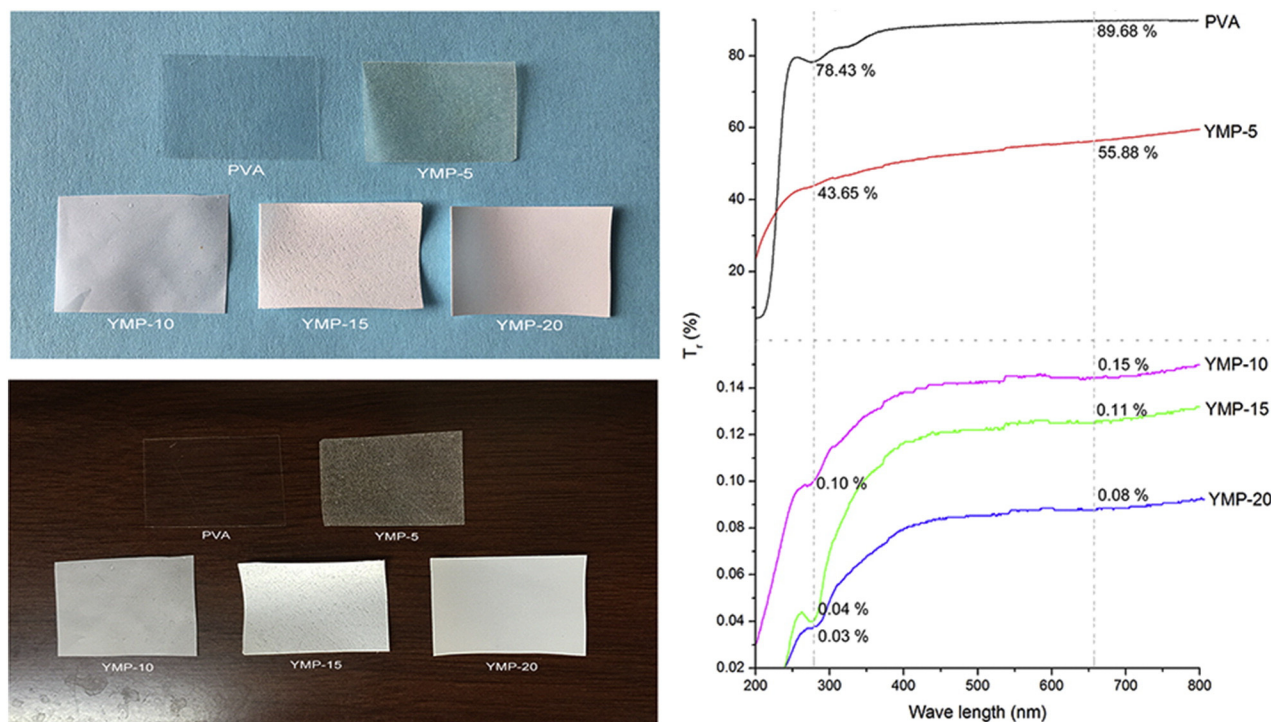


**Fig. 8.** Photographs and visible-light transmittance curves of the films.

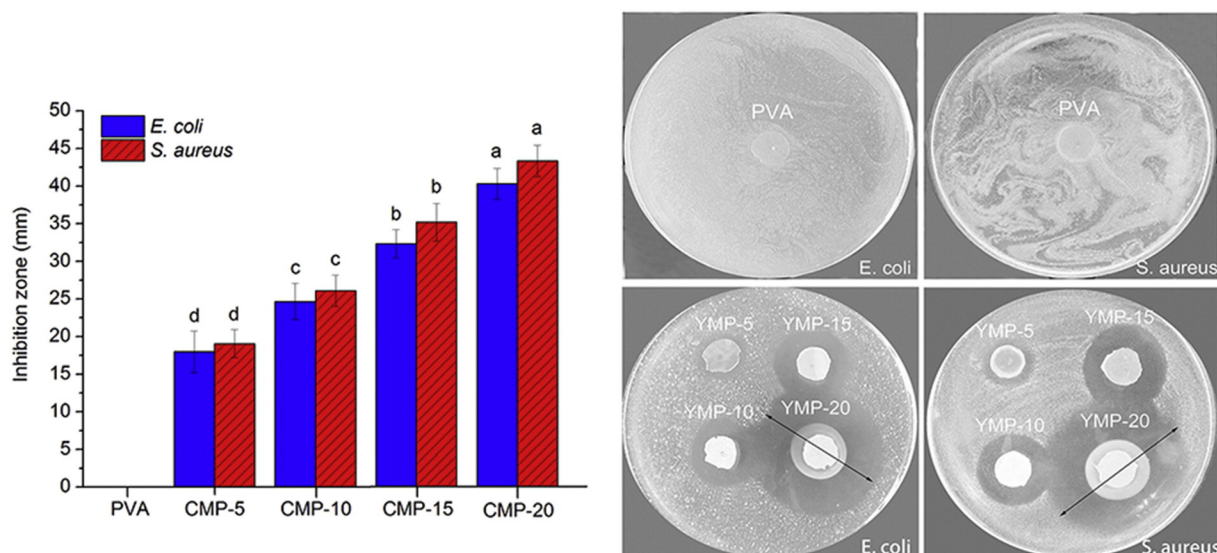


Fig. 9. Activities of the composite films against *E. coli* and *S. aureus*, as determined by the disc diffusion method. Different letters indicate significant differences among films as determined by Duncan's multiple-range tests ( $p < 0.05$ ).

ammonium derivatives are used extensively as bactericides. The mechanism of their antibacterial activity is hypothesized to arise from the electrostatic interaction between  $\text{-NH}_3^+$  groups of YM and phosphoryl groups of phospholipid components of cell membranes [47]. This interaction disrupts bacterial cell walls and kills planktonic microorganisms [48]. Our results show that the antibacterial activity of the YMP film markedly increased as the YM content increased from 5 to 20 wt.% because of the presence of more ammonium groups in the blend film. The activity of the samples against *S. aureus* was stronger than against *E. coli*. This difference in antibacterial activity is related to the difference in structural and chemical composition of their cell membranes [49]. In particular, *S. aureus* is more susceptible to antibiotics than is *E. coli* because the latter has a relatively impermeable lipid-based outer membrane [50].

#### 4. Conclusion

PVA/YM blend films were prepared from a homogeneous system. The effects of YM content on the properties of the films were evaluated. XRD analysis showed that PVA/YM composite films had higher crystallinity than did pure PVA film, thus revealing that YM could strongly interact with PVA through hydrogen bonding. The composite films showed high tensile strength, high thermostability, and significant water vapor barrier property. However, they had poor flexibility, low OP, and low light transmission compared with pure PVA film. They showed notable activity against Gram-positive (*S. aureus*) and Gram-negative (*E. coli*) bacteria. The composite films in this work may be potential alternatives to plastic films commonly used in packaging and in other applications.

#### Acknowledgments

This work was supported by the National Natural Science Foundation of China (31470612) and the Fundamental Research Funds of the Central Universities (2572015A05).

#### References

[1] N. Lavoine, I. Desloges, A. Dufresne, J. Bras, Carbohydr. Polym. 90 (2012) 735–764.  
 [2] J.Q. Zhao, X.M. Zhang, R. Tu, C.H. Lu, X. He, W. Zhang, Cellulose 21 (2014) 1859–1872.

[3] J.H. Pang, M. Wu, Q.H. Zhang, X. Tan, F. Xu, X.M. Zhang, R.C. Sun, Carbohydr. Polym. 121 (2015) 71–78.  
 [4] H.J. Geng, Z.W. Yuan, Q.R. Fan, X.N. Dai, Y. Zhao, Z.J. Wang, M.H. Qin, Carbohydr. Polym. 102 (2014) 438–444.  
 [5] T.-W. Lee, Y.G. Jeong, Carbohydr. Polym. 133 (2015) 456–463.  
 [6] M. Soheilimoghaddam, M.U. Wahit, N.I. Akos, Mater. Lett. 111 (2013) 221–224.  
 [7] R. Li, L.N. Zhang, M. Xu, Carbohydr. Polym. 87 (2012) 95–100.  
 [8] Y. Mao, J. Zhou, J. Cai, L. Zhang, J. Membr. Sci. 279 (2006) 246–255.  
 [9] D. Ruan, J. Membr. Sci. 241 (2004) 265–274.  
 [10] R.D. Pavaloiu, A. Stoica-Guzun, M. Stroescu, S.I. Jinga, T. Dobre, Int. J. Biol. Macromol. 68 (2014) 117–124.  
 [11] M.S. Peresin, Y. Habibi, A.H. Vesterinen, O.J. Rojas, J.J. Pawlak, J.V. Seppala, Biomacromolecules 11 (2010) 2471–2477.  
 [12] J.-F. Su, Z. Huang, C.-M. Yang, X.-Y. Yuan, J. Appl. Polym. Sci. 110 (2008) 3706–3716.  
 [13] O. Kukhareno, J.-F. Bardeau, I. Zaets, L. Ovcharenko, O. Tarasyuk, S. Porhyn, I. Mischenko, A. Vovk, S. Rogalsky, N. Kozrovska, Eur. Polym. J. 60 (2014) 247–254.  
 [14] T. Maneerung, S. Tokura, R. Rujiravanit, Carbohydr. Polym. 72 (2008) 43–51.  
 [15] N.-T. Nguyen, J.-H. Liu, J. Taiwan Inst. Chem. Eng. 45 (2014) 2827–2833.  
 [16] Y.-M. Jeon, H.-S. Lee, D.J. Jeong, H.-K. Oh, K.-H. Ra, M.-Y. Lee, Life Sci. 124 (2015) 56–63.  
 [17] Y.B. Zhang, X.Y. Liu, Y.F. Wang, P.P. Jiang, S.Y. Quek, Food Control 59 (2016) 282–289.  
 [18] D. Roy, J.S. Knapp, J.T. Guthrie, S. Perrier, Biomacromolecules 9 (2008) 91–99.  
 [19] Y. Qi, J. Li, L. Wang, Ind. Crop. Prod. 50 (2013) 15–22.  
 [20] Y.B. Song, J. Zhang, W.P. Gan, J.P. Zhou, L.N. Zhang, Ind. Eng. Chem. Res. 49 (2010) 1242–1246.  
 [21] T.-S. Kim, T. Hirao, I. Ikeda, J. Am. Oil Chem. Soc. 73 (1996) 67–71.  
 [22] J. Zhou, L. Zhang, J. Cai, H. Shu, J. Membr. Sci. 210 (2002) 77–90.  
 [23] Y.B. Song, Y.X. Sun, X.Z. Zhang, J.P. Zhou, L.N. Zhang, Biomacromolecules 9 (2008) 2259–2264.  
 [24] L. Wang, J. Li, Ind. Crop. Prod. 42 (2013) 153–158.  
 [25] S. Abbasizadeh, A.R. Keshtkar, M.A. Mousavian, Chem. Eng. J. 200 (2013) 161–171.  
 [26] X. Zhang, J. Tan, X. Wei, L. Wang, Carbohydr. Polym. 92 (2013) 1497–1502.  
 [27] D.Y. Hu, H.X. Wang, L.J. Wang, LWT – food, Sci. Technol. 65 (2016) 398–405.  
 [28] M.S. Peresin, Y. Habibi, J.O. Zoppe, J.J. Pawlak, O.J. Rojas, Biomacromolecules 11 (2010) 674–681.  
 [29] N.E. Miri, M.E. Achaby, A. Fihri, M. Larzek, M. Zahouily, K. Abdelouahdi, A. Barakat, A. Solhy, Carbohydr. Polym. 137 (2016) 239–248.  
 [30] A. Cano, E. Fortunati, M. Cháfer, J.M. Kenny, A. Chiralt, C. González-Martínez, Food Hydrocoll. 48 (2015) 84–93.  
 [31] A.N. Frone, D.M. Panaitescu, D. Donescu, C. Radovici, M. Ghiurea, M.D. Iorga, Mater. Plast. 48 (2011) 138–143.  
 [32] S.L. Xiao, R.A. Gao, L.K. Gao, J. Li, Carbohydr. Polym. 136 (2016) 1027–1034.  
 [33] D.M. Panaitescu, A.N. Frone, M. Ghiurea, I. Chiulan, Ind. Crop. Prod. 70 (2015) 170–177.  
 [34] J. Cai, J.Y. Chen, Q. Zhang, M. Lei, J.R. He, A.H. Xiao, C.J. Ma, S. Li, H.G. Xiong, Carbohydr. Polym. 140 (2016) 238–245.  
 [35] S.S. Laxmeshwar, S. Viveka, D.J. Madhu Kumar, Dinesha, R.F. Bhajanthri, G.K. Nagaraja, J. Macromol. Sci. A 49 (2012) 639–647.  
 [36] A.L. Brody, B. Bugusu, J.H. Han, C.K. Sand, T.H. McHugh, J. Food Sci. 73 (2008) R107–R116.  
 [37] E. Ayrançi, S. Tunc, Food Chem. 80 (2003) 423–431.  
 [38] M.B. Perez-Gago, J.M. Krochta, J. Food Sci. 66 (2001) 705–709.

- [39] T.H. McHugh, C.C. Huxsoll, J.M. Krochta, *J. Food Sci.* 61 (1996) 88–91.
- [40] R. Sothornvit, N. Pitak, *Food Res. Int.* 40 (2007) 365–370.
- [41] W. Thakhiew, S. Devahastin, S. Soponronnarit, *J. Food Eng.* 119 (2013) 140–149.
- [42] Q. Yang, H. Fukuzumi, T. Saito, A. Isogai, L. Zhang, *Biomacromolecules* 12 (2011) 2766–2771.
- [43] B. Ghanbarzadeh, H. Almasi, *Int. J. Biol. Macromol.* 48 (2011) 44–49.
- [44] Z. Shen, M. Ghasemlou, D.P. Kamdem, *J. Appl. Polym.* 41354 (2015) 1–8.
- [45] Á. Perdonés, M. Vargas, L. Atarés, A. Chiralt, *Food Hydrocoll.* 36 (2014) 256–264.
- [46] S.Y. Wang, J.L. Ren, W.Q. Kong, C.D. Gao, C.F. Liu, F. Peng, R.C. Sun, *Cellulose* 21 (2014) 495–505.
- [47] H. Liu, Y.M. Du, X.H. Wang, L.P. Sun, *Int. J. Food Microbiol.* 95 (2004) 147–155.
- [48] M.M. Fernandes, A. Francesko, J. Torrent-Burgues, F.J. Carrion-Fite, T. Heinze, T. Tzanov, *Biomacromolecules* 15 (2014) 1365–1374.
- [49] S. Azizi, M. Ahmad, M. Mahdavi, S. Abdolmohammadi, *Bioresources* 8 (2013) 1841–1851.
- [50] Z. Shariatinia, M. Fazli, *Food Hydrocoll.* 46 (2015) 112–124.